The effect of inter-layer diffusion on magnetic exchange spring behaviour

2008 J. Phys.: Condens. Matter 20 125223

(http://iopscience.iop.org/0953-8984/20/12/125223)

IOP PUBLISHING JOURNAL OF PHYSICS: CONDENSED MATTER

J. Phys.: Condens. Matter **20** (2008) 125223 (7pp) doi:10.1088/0953-8984/20/12/125223

The effect of inter-layer diffusion on magnetic exchange spring behaviour

G J Bowden[1,3], K N Martin[1], A Fox[1], B D Rainford[1], R C C Ward[2] and P A J de Groot[1]

[1] School of Physics and Astronomy, University of Southampton, SO17 1BJ, UK
[2] Clarendon Laboratory, University of Oxford, Parks Road, Oxford, OX1 3PU, UK

E-mail: gjb@phys.soton.ac.uk

Received 7 December 2007, in final form 8 February 2008
Published 3 March 2008
Online at stacks.iop.org/JPhysCM/20/125223

Abstract
The effect of inter-layer diffusion between the magnetically hard and soft layers in magnetic exchange spring systems is examined, using 1D and 2D models. It is shown that diffusion across the hard/soft interfaces leads to an increase in the bending field B_B. This increase eventually saturates when the bending field B_B and the coercivity B_C merge. Moreover, if the increase in the bending field B_B is large enough, the nature of the magnetic reversal can be affected. This behaviour is illustrated using a YFe_2 dominated $YFe_2/DyFe_2$ exchange spring system. In this case the 1D model predicts that inter-layer diffusion can drive a magnetic phase change, from negative to positive coercivity. Discrete 2D model calculations of inter-layer diffusion are also presented and discussed. The latter support the predictions of the 1D model. Finally, while the emphasis is on atomic diffusion, some comments are made concerning interface roughness.

(Some figures in this article are in colour only in the electronic version)

1. Introduction

YFe_2/RFe_2 magnetic superlattice films (where R is a rare earth), grown by molecular beam epitaxy (MBE), make excellent model systems in which to study the properties of magnetic exchange springs (Dumesnil *et al* 2000, Sawicki *et al* 2000, Bentall *et al* 2003b, 2003b, Martin *et al* 2006). In these superlattices, the RFe_2 layers form *hard pinning* layers, allowing magnetic exchange springs to be set up in the *soft* YFe_2 layers. In particular, it has been shown that the bending field B_B (the onset of the magnetic exchange spring) scales as $1/d^2$, where d is the thickness of the YFe_2 layers (Sawicki *et al* 2000). However, recently, both x-ray and high resolution TEM studies have indicated that the interface between the RFe_2 and YFe_2 layers is not perfectly flat, but exhibits a degree of either inter-layer diffusion and/or interface roughness (Bentall *et al* 2003b). For example, in the multilayer [$DyFe_2$-70 Å/YFe_2-30 Å] × 60, the interface width amounts to ∼9 Å. However, it can be much larger, up to ∼30 Å (see Bentall *et al* 2003b, table 3). Further, given that experiments have been published on $DyFe_2/YFe_2$ superlattices with layer thicknesses ∼30–50 Å (Dumesnil *et al* 2005a, 2005b and Fitzsimmons *et al* 2006), it is important to assess the effect of interface broadening on magnetic behaviour.

In this paper, an attempt is made to address some of these questions by modelling the effect of inter-layer width on the magnetic properties of model $DyFe_2/YFe_2$ multilayer films. As a first approach, it will be assumed that the transition width is due solely to atomic diffusion across the interface, for small length scales ∼50 Å. In general, we believe that correlated roughness over in-plane larger length scales, say ∼1000 Å, will have only a small effect on magnetic exchange spring behaviour.

In the first instance, calculations were performed using a 1D exchange spring model (Bowden *et al* 2000), Bowden *et al* 2008, but modified to include spatial inter-diffusion of the Dy/Y ions. The latter is included as a gradual change in both anisotropy and Zeeman interactions, across the interface. For small inter-diffusion, the effect on the magnetic properties of $DyFe_2$ dominated multilayers is found to be relatively modest. But in YFe_2 dominated samples, inter-layer diffusion can bring about fundamental changes in the very character of the M–B_{app} loop. In general terms, the change in magnetic behaviour can be ascribed to a stiffening of the exchange spring, as the Dy

[3] Author to whom any correspondence should be addressed.

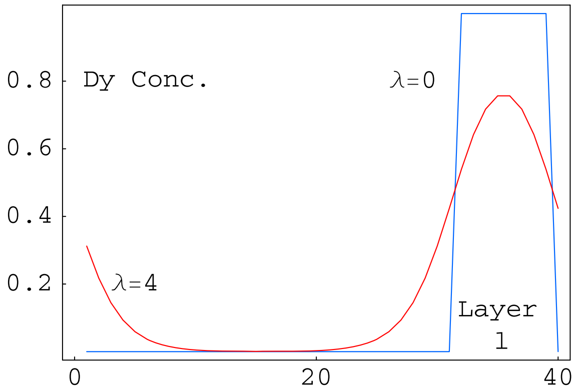

Figure 1. The distribution of Dy ions as a function of the layer number l. Blue line, no diffusion. Red line, with diffusion.

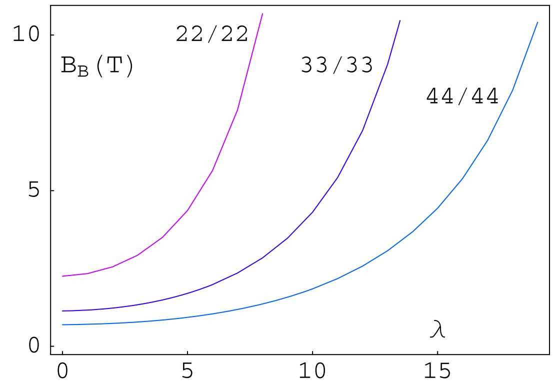

Figure 2. The calculated bending fields B_B as a function of the diffusion parameter λ, for three superlattices $N_{DyFe2}/N_{YFe2} = 22/22$, 33/33 and 44/44, with cyclic boundary conditions. These correspond roughly to 80 Å/80 Å, 120 Å/120 Å, 160 Å/160 Å, respectively.

ions penetrate into the soft YFe_2 layers. Similar behaviour is also found in the 2D model. However, in the latter, it is possible to simulate diffusion in a truly discrete way. Simplified 2D cases are presented and discussed, which exhibits short-range disorder at the interface, and are consistent with the interface thickness of Bentall *et al* (2003b).

Finally, to avoid duplication, this paper should be read in conjunction with that of Bowden *et al* 2008, which gives full details of the 1D, 2D and 3D formulation of the magnetic exchange spring model used in this paper. In particular, the simulation cell for the RFe_2 Laves compounds is set at $(a/2)^3$, where a is the size of the unit cell, $a = 7.325$ Å for $DyFe_2$. This cell volume corresponds to one RFe_2 formula unit.

2. Model of inter-layer diffusion

As mentioned earlier, details of the Dy/Y composition across the $DyFe_2/YFe_2$ interfaces can be found in (Bentall *et al* 2003b). In their fit to the x-ray data, the transition region is characterized by a single parameter λ, as illustrated schematically in figure 1. Specifically, the concentration $c(l)$ of Dy ions per mono-layer l is given by:

$$c(l) = 1 - \frac{1}{2}\left\{\sum_{S=1}^{N-2} \tanh\left[\frac{l + 0.5 - \bar{\Lambda}S}{\lambda}\right] - \sum_{S=0}^{N-1} \tanh\left[\frac{l + 0.5 - n_1 - \bar{\Lambda}S}{\lambda}\right]\right\} \quad (1)$$

where (i) $n_1(n_2)$ are the number of YFe_2 ($DyFe_2$) mono-layers, respectively, (ii) $\bar{\Lambda}$ ($= n_1 + n_2$) is the bi-layer thickness, again in mono-layers, (iii) N is the total number of bi-layers in the film, and (iv) λ is the diffusion width, again in mono-layers. However, since we make use of cyclic boundary conditions, we set N large and odd, and select the middle bi-layer $c(l)$ for our purposes. In this way, the normalization condition:

$$\sum_{l=1}^{\bar{\Lambda}} c(l) = n_2 \quad (2)$$

is satisfied, regardless of the value of the diffusion parameter λ. Note that the model is continuous in that it assumes the existence of partial concentrations of Dy and Y atoms, across the interface. Thus the effective Dy magnetic moment and axial anisotropy K_A per layer l are given by $c(l)\mu_{Dy}$ and $c(l)K_A$, respectively. In essence therefore, the model can be described as the 'average' of line upon line of $YFe_2/DyFe_2$ strings, perpendicular to the plane of the film. Thus the model is incapable of distinguishing between diffusion and surface roughness. In section 5, we shall re-address this issue, this time using a discrete diffusion model in 2D.

Finally, we note that for the data shown in figure 1, $\lambda = 4$ corresponds roughly to the interface width in mono-layers, as defined by the 20% and 80% levels of the maximum Dy concentration.

3. 1D model calculations for $DyFe_2$ dominated multilayers

Initially, calculations were performed for three multilayers $N_{YFe2}/N_{DyFe2} = 22/22$, 33/33 and 44/44. They correspond, approximately, to the multilayer films [80 Å-YFe_2/80 Å-$DyFe_2$], [120 Å-YFe_2/120 Å-$DyFe_2$], and [160 Å-YFe_2/160 Å-$DyFe_2$]. In these structures the DyFe2 magnetization is dominant.

The calculated bending fields B_B, as a function of the inter-diffusion width λ, can be seen in figure 2. From this data it is clear that the bending field B_B increases as soon as diffusion of Dy into the YFe_2 layer occurs. From table 3 of Bentall *et al* (2003b), we find 9 Å $\leqslant \lambda \leqslant$ 39 Å, with an average $\lambda \sim 22$ Å. If we set $\lambda = 6$ mono-layers (∼22 Å), the rise in B_B amounts to 50.4%, 74.5% and 150.8% for the 44/44, 33/33 and 22/22 superlattices, respectively. In summary, for very thick YFe_2 layers (>200 Å) the increase in B_B is relatively small. But as the thickness of the YFe_2 layers is reduced, the increase in B_B becomes pronounced.

Physically, we interpret these results as follows. For small Dy inter-penetration the effect on B_B is minimal. This can be viewed as the cancellation of two effects. Initially, the spring *stiffens* as Dy ions move into the YFe_2 layer. But this is somewhat mitigated by the reduction of the *pinning force* at the $DyFe_2$ edge. However as more and more Dy ions migrate into

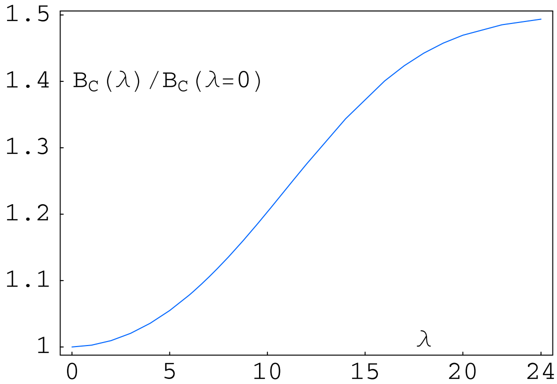

Figure 3. The normalized coercivity B_C ($= 4.955$ T for $\lambda = 0$), as a function of the diffusion parameter λ, for the superlattice $N_{DyFe2}/N_{YFe2} = 22/22$ with cyclic boundary conditions.

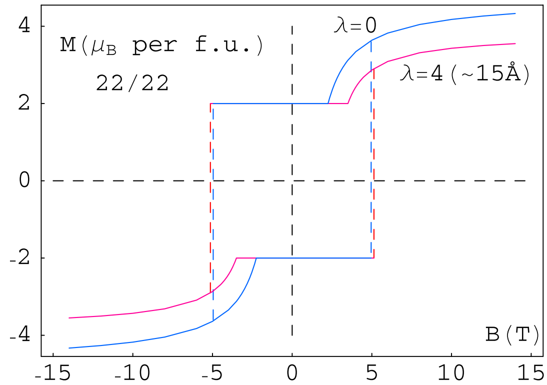

Figure 4. The calculated magnetic loops for the superlattice $N_{DyFe2}/N_{YFe2} = 22/22$ (~80 Å/80 Å), for $\lambda = 0$ and 4 (~15 Å), with cyclic boundary conditions.

the YFe_2 layers, the so-called soft layer becomes increasingly more *rigid*, due to both the anisotropy *and* Zeeman interactions of Dy ions. Since the Dy moments within the YFe_2 layers are already pointing in the direction of the applied field, they act to suppress the creation of magnetic exchange springs. Indeed, in the limit of total inter-diffusion, the *soft* layer disappears, and the concept of a bending field B_B becomes meaningless.

In addition to providing predictions for the bending field B_B, the model can also be used to calculate the coercivity B_C. Of course, in view of Brown's paradox (Brown 1963, Cullity 1972), such values should be treated with caution. Nevertheless, for comparative purposes (Bowden *et al* 2003) we have calculated B_C as a function of the inter-diffusion parameter λ. The results, summarized in figure 3, show that the effect of inter-diffusion on B_C is much less than that on B_B. But note that as λ approaches $N = 22$ mono-layers, i.e. the width of the YFe_2 layers, the coercivity saturates, reaching a ~50% increase on the diffusion free value $B_C(\lambda = 0)$. For such values of λ, the distribution of the Dy ions is almost uniform throughout the $YFe_2/DyFe_2$ multilayer. Thus as λ is increased, the bending field B_B and the coercivity B_C merge into each other.

Finally, in figure 4 we show the calculated magnetization loops for the multilayer film $N_{DyFe2}/N_{YFe2} = 22/22$, for $\lambda = 0$ and 4 (~15 Å), respectively. Here the model predicts that inter-layer diffusion will cause (i) an increase in the bending field B_B, (ii) a smaller increase in the coercivity B_C, and (iii) a fall in the saturation magnetization M_S. Points (i) and (iii) can be attributed to the *stiffening* of the magnetic exchange spring, making it less responsive to applied magnetic fields. Further, as λ is increased, the contribution to the magnetization from the exchange spring will become smaller and smaller, reaching ~zero for $\lambda \geqslant 22$. The loop is then square, because the bending field B_B and the coercivity B_C have coalesced.

In summary therefore, for $DyFe_2$ dominated samples the effect of diffusion is minimal, provided λ/N_{YFe2} is relatively small, say less than 10%. But as the ratio is increased, the character of the M versus B loop can change substantially. Clearly diffusion will have important implications for multilayers with relatively small thicknesses of YFe_2 layers. In the next section, we turn our attention to YFe_2 dominated multilayers.

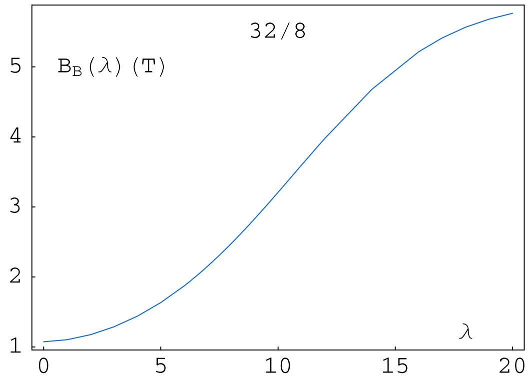

Figure 5. The calculated bending fields B_B as a function of the diffusion parameter λ, for the superlattice $N_{YFe2}/N_{DyFe2}/ = 32/8$, with cyclic boundary conditions.

4. 1D model calculations for YFe_2 dominated multilayers

As mentioned earlier, XMCD measurements on the multilayer [30 Å-$DyFe_2$/120 Å-YFe_2] × 22 and [50 Å-$DyFe_2$/200 Å-YFe_2] × 13 have been reported by Dumesnil *et al* (2005a), (2005b). In an attempt to simulate results for the former, we have performed calculations for the multilayer $N_{DyFe2}/N_{YFe2} = 8/32$.

The calculated bending fields for the 32/8 superlattice can be seen in figure 5. Here, it will be observed that when diffusion parameter λ is ~4 (~15 Å) the bending field transition has increased by 34%. But while this is appreciable, it might appear that the effect of inter-diffusion on the magnetic loop is again likely to be minimal. However when we come to calculate the full magnetic loop an entirely different picture emerges.

The calculated magnetization curve for $\lambda = 0$ can be seen in figure 6. It will be observed that the magnetization loop is characterized by a negative coercivity: a classic feature of a YFe_2 dominated multilayer (Beaujour *et al* 2001).

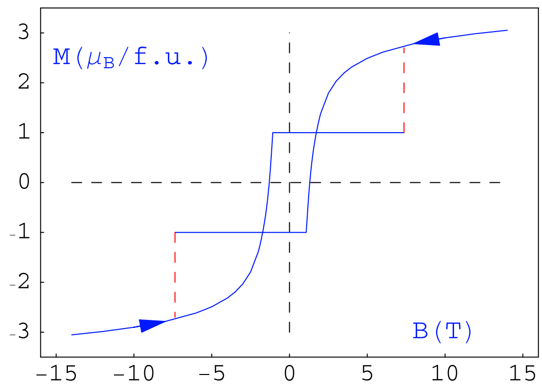

Figure 6. The calculated magnetization loop for the superlattice $N_{YFe2}/N_{DyFe2}/32/8$, for $\lambda = 0$ and cyclic boundary conditions.

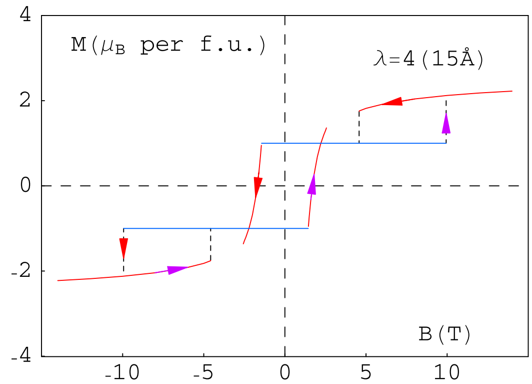

Figure 7. The calculated magnetization loop for the superlattice $N_{YFe2}/N_{DyFe2} = 32/8$, for $\lambda = 4$ (∼15 Å). The straight blue lines represent simple AF states, while the curved red lines indicate the presence of exchange springs. See the text for a discussion of the gap between the high and low field exchange spring states.

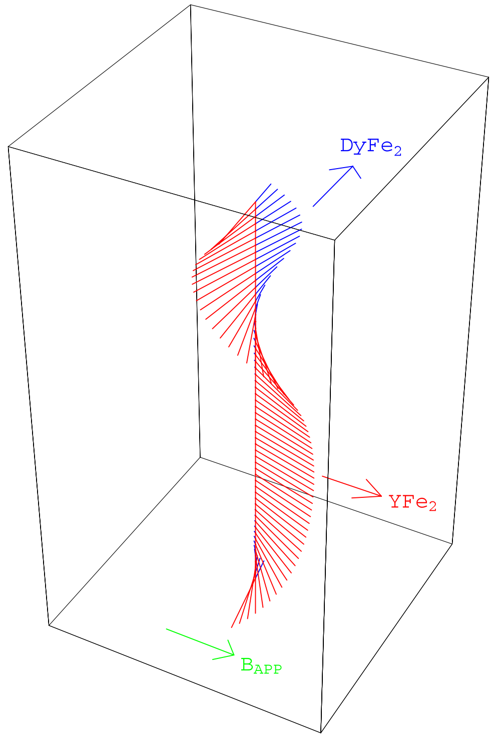

Figure 8. A schematic drawing of an exchange spring driven spin-flop state (ESDSF) for $N_{YFe2}/N_{DyFe2}/ = 32/8$, with $\lambda = 4$, and field $B = 5$ T applied along the easy axis. Note that the Fe moments (red online) in the YFe_2 layer point mainly in the direction of the applied magnetic field while in the $DyFe_2$ layers the Dy moments (blue online) point mainly at right angles to the applied field, along a hard axis.

However when the same calculations are carried out for $\lambda = 4$ (∼15 Å), an entirely different picture emerges. The results shown in figure 7 reveal that the coercivity is now positive.

The loop can be described as follows. In a large positive field >9.94 T, the stable state is a magnetic exchange spring (red line) with the Fe moments in the YFe_2 layer pointing mainly in the direction of the magnetic field. At the same time, the Dy moments (and their Fe moments) are aligned mainly at right angles to the applied field. An example can be seen in figure 8. We shall refer to this state as an *exchange spring driven spin-flop* (ESDSF). Such ESDSF transitions have been observed in the $ErFe_2/YFe_2$ system by (Martin *et al* 2006). Note that the ESDSF state of figure 8 differs from that of Martin *et al*, in that (i) inter-diffusion is responsible for the transition, (ii) the spins are in-plane (Dy) rather than out-plane (Er). In the model $DyFe_2/YFe_2$ system under discussion, the spin-configuration *jumps* from a simple AF-state into a planar ESDSF state (similar to that of figure 8) at the spin-flop field $B_{SF}(= 9.94$ T).

Subsequently, as the field is reduced below 4.57 T, the spin-configuration snaps into a simple AF-state (straight blue line in figure 7) with the all Fe moments pointing to the right and all the Dy moments pointing to the left. This simple AF-state is maintained, as the field is reduced through zero, until the bending field transition at $B_B = -1.44$ T. Beyond this transition, a soft magnetic exchange spring is set up in the YFe_2 layer, producing an average Fe moment parallel to the applied field. However, this soft magnetic exchange spring is only stable between −1.44 T and −2.56 T. Moreover at −2.56 T, an examination of the spin-configuration reveals that the Dy spins are on the edge of being turned over to point in an opposite direction to the applied field i.e. to adopt the reverse AF-state. Finally, at fields between −2.4 T and −2.56 T, the exchange spring state lies in a localized energy minimum, with an energy higher than that of the AF-state. Consequently, at approximately −2.5 T, the Dy and Fe spins suddenly switch over, and the reverse AF-state now becomes the new stable spin-configuration. Note that this behaviour is quite unlike that of figure 6, where the magnetic exchange spring remains stable at all fields beyond the bending field transition.

From the above discussion, it is clear that inter-layer diffusion has the potential to drive changes in the character of the magnetic hysteresis loop. The prime reason for the changeover in character of the two magnetization loops lies in the *stiffening* of the soft YFe_2 layer. An exchange spring will only form if the loss in exchange and anisotropy energy is offset by a concomitant gain in Zeeman energy. Clearly this becomes more difficult in the case of *rigid* exchange springs.

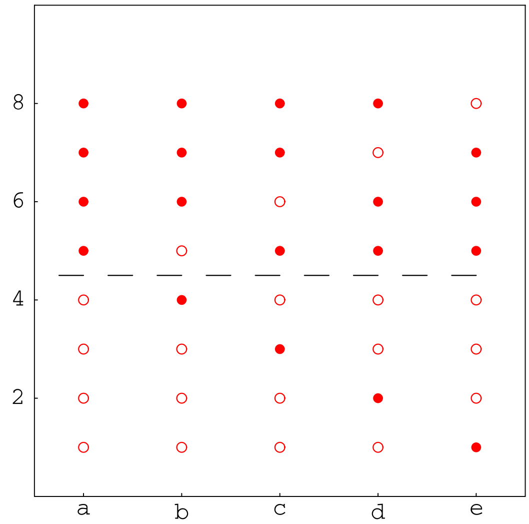

Figure 9. The five possibilities for inter-layer diffusion (see the text). The full (empty) circles represent Dy(Y) ions, respectively. The dashed line represents the interface.

This point is also evident from a comparison of the saturated magnetic moments in figures 6 and 7. In the presence of inter-diffusion ($\lambda = 4$), the magnetic moment is some 27% lower, in a field of 14 T.

This completes our discussion of the 1D model, and we turn now to 2D models of discrete as opposed to continuous diffusion.

5. Discrete models of diffusion in 2D

In practice, computational requirements place severe limitations on what can be achieved. In the first place therefore, we have chosen a simplified 2D diffusion model, involving 15 strings of $N_{\mathrm{YFe2}}/N_{\mathrm{DyFe2}} = 32/8$, i.e. a total of 600 spins. The reason for choosing the number 15 will soon become apparent.

The inter-layer diffusion model that we have adopted, is shown schematically in figure 9.

From this diagram, it will be seen that maximum diffusion of a Dy/Y ion across the interface (dotted line) has been set at 4 mono-layers (∼15 Å). Moreover, for each of the five columns (a)–(e) the diffusing Y and Dy ions are equally disposed about the interface. Thus the centre of the interface remains unchanged. Secondly, we ascribe the following probabilities to each of the five columns shown in figure 9: that no diffusion takes place 'a' (5/15), that the Dy/Y hop one mono-layer across the interface 'b' (4/15), etc., down to four mono-layers 'e' (1/15). Hence 15 $YFe_2/DyFe_2$ strings are required to preserve normality. Thirdly, the 15 possibilities have been chosen at random, both for the top and bottom interfaces. The sequence actually used is given by:

$$\begin{aligned} &\text{Top layer} \quad \{a, b, b, a, b, d, c, e, a, d, c, a, a, c, b\} \\ &\text{Bottom layer} \ \{c, a, b, c.c, d, e, b, a, b, b, a, d, a, a\}. \end{aligned} \tag{3}$$

The resultant magnetization loop was found to be very similar that of figure 6, for the case of no inter-diffusion. The bending field B_B increased from 1.074 to 1.188 T, while the magnetization at 14 T fell by some 15%. Clearly, more inter-layer diffusion is required to drive a potential switch from negative to positive coercivity.

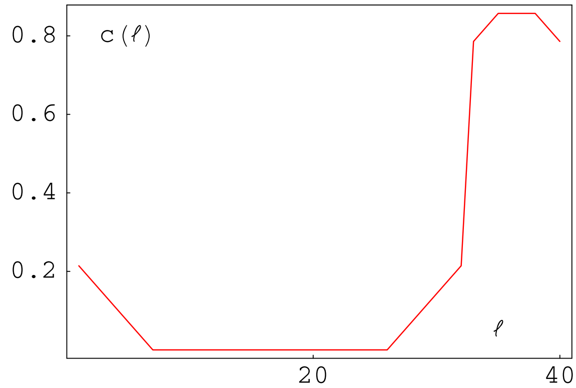

Figure 10. The concentration function $c(l)$ per layer l, for the discrete 2D diffusion model, but normalized to a 1D chain of $N_{\mathrm{YFe2}}/N_{\mathrm{DyFe2}}/ = 32/8$ moments.

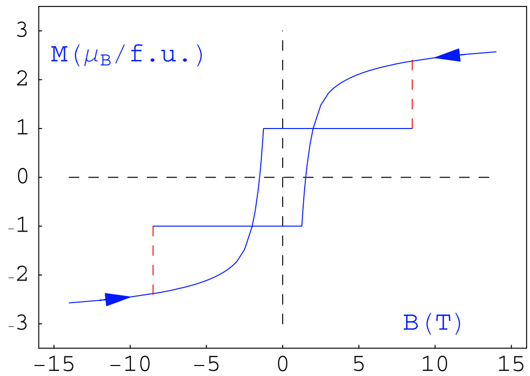

Figure 11. The calculated 2D magnetization curve, for 28 strings of $N_{\mathrm{YFe2}}/N_{\mathrm{DyFe2}}/ = 32/8$, with (i) the diffusion pattern summarized in equation (4), and (ii) cyclic boundary conditions. The bending field transition $B_B = 1.255$ T.

A second calculation was carried out for a maximum diffusion of 6 mono-layers (∼22 Å). This involved a set of 28 strings, involving a total of 1120 spins. The sequence used for the top and bottom layers is given by:

$$\begin{aligned} &\text{Top layer} \ \big\{c, f, a, d, d, c, e, d, f, b, b, b, a, a, a, c, \\ &\quad c, g, a, d, a, c, b, a, b, e, b, e\big\} \\ &\text{Bottom layer} \ \big\{d, a, b, e, d, d, a, b, c, d, e, f, a, c, c, a, g, \\ &\quad a, b, a, c, b, a, c, f, b, e, b\big\}. \end{aligned} \tag{4}$$

The average distribution population, normalized to a single string, can be seen in figure 10. It will be seen from a comparison figures 1 and 10, that the discrete model is reasonably consistent with the continuous model of (Bentall *et al* 2003b).

The calculated magnetization loop for this model can be seen in figure 11. However, once again the loop exhibits negative coercivity. The new bending field $B_B = 1.255$ T, with an increased coercivity B_C of 8.498 T. It is clear therefore that

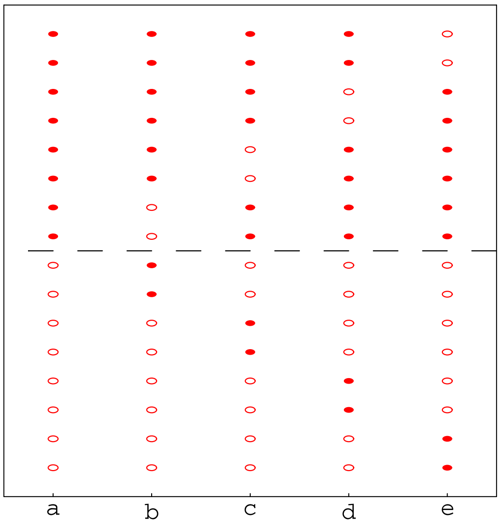

Figure 12. The two-atom jump model. The full (empty) circles represent Dy(Y) ions, respectively. The dashed line represents the interface.

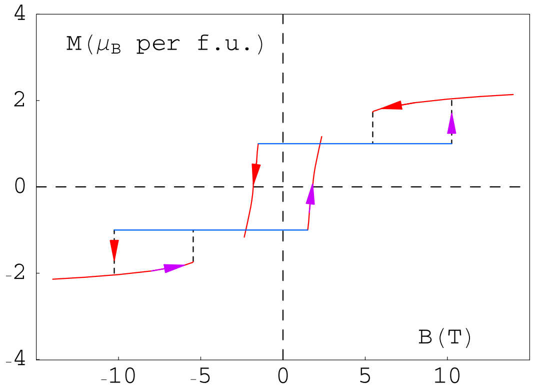

Figure 13. The calculated 2D magnetization curve, for 15 strings of $N_{YFe2}/N_{DyFe2}/ = 32/8$, with the diffusion pattern summarized in equation (5) and figure 12. Cyclic boundary conditions have been used. The bending field transition $B_B = 1.502$ T.

while inter-layer diffusion has increased the bending field B_B, it falls short of the 1.44 T of the continuous model of figure 7. In this case therefore, an ESDSF transition does not take place.

Nonetheless, it is possible to simulate the 2D results shown in figure 11, with the 1D model. If we set $\lambda = 3$, we find $B_B = 1.288$ T, close to that of figure 10. Further, the 1D model predicts that the coercivity is still negative. Thus the results obtained using a 1D exchange spring model, with a continuous distribution, are similar to those of the 2D model with a discrete distribution.

To increase the bending field B_B still further, it is necessary to extend the diffusion, say out to 8 mono-layers. This in turn will involve a set of 45 strings of $YFe_2/DyFe_2$ moments (3600 spins), beyond the present limit of our calculations. However, further progress can be made by adopting the 'two-atom' jump model shown in figure 12.

From a comparison of figures 9 and 12, it will be observed that in the latter two atoms, as opposed to one atom, now jump across the interface. Moreover the R atoms can migrate up to 8 atomic spacings, away from the interface. Once again five possibilities a–e are considered, leading to a set of 15 strings, well within computational possibilities. The calculations were carried out with:

$$\begin{aligned} &\text{Top layer} \quad \{b, c, d, a, d, b, a, a, c, b, e, a, c, a, b\} \\ &\text{Bottom layer} \ \{d, a, b, b, e, c, c, c, a, a, a, d, b, a, b\}. \end{aligned} \qquad (5)$$

The bending field transition was found to be 1.502 T, above the bending field transition of 1.44 T, for the 1D results of figure 7. Consequently, the magnetization loop should now be characterized by a positive coercive field. The calculated magnetization loop can be seen in figure 13, which shows that this is indeed the case. For discrete diffusion therefore, ESDSF transitions can take place. Note also that the magnetization loops of figure 7 (1D model) and figure 13 (2D model) are very similar.

Finally, it should be acknowledged that we are not the only authors to suggest that the properties of magnetic multilayers can be changed by encouraging say the diffusion of hard magnetic layers into their softer counterparts. Jiang *et al* (2004, 2005) and Choi *et al* (2007) have argued that diffusion via thermal processing in SmCo/Fe films can have beneficial effects, in improving the $(B–H)_{MAX}$ of exchange spring nano-composite permanent magnets.

6. Discussion and conclusions

In this paper, the effect of inter-layer diffusion on the magnetic properties of $DyFe_2/YFe_2$ magnetic multilayers has been investigated using (i) the continuous diffusion model of Bentall *et al* (2003a, 2003b) within a 1D magnetic exchange spring model, and (ii) a 2D magnetic exchange spring model, but this time with discrete diffusion. Both models allow the key-physics associated with inter-layer diffusion to be identified. Inter-layer diffusion increases the rigidity of the magnetic exchange springs, which in turn leads to concomitant changes in the magnetization loop. In particular, for YFe_2 dominated superlattices, there is the potential for dramatic changes in the nature of magnetic reversal, provided the increase in the bending field B_B is large enough. This increase can be brought about by inter-layer diffusion, small scale surface roughness, or say graded deposition. Finally, what actually happens at the interfaces in MBE grown RFe_2/YFe_2 multilayers needs further investigation. If the interfaces in $DyFe_2/YFe_2$ multilayers are atomically sharp to within ±2 Å (see Fitzsimmons *et al* (2006), section II and figure 2), the effects will be minor. However, if the compositional profiles deduced from x-ray analysis (Bentall *et al* 2003b) are correct, the magnetization processes in YFe_2 dominated samples will be affected dramatically. Clearly there is a need for more precise interface studies in $REFe_2/YFe_2$ superlattices, with the spotlight on separating diffusion from interface roughness, correlated roughness etc, on various length scales.

Acknowledgments

This work has been supported by EPSRC. The authors would also like to acknowledge useful conversations with R A Cowley.

References

Beaujour J-M L, Bowden G J, Gordeev S, de Groot P A J, Rainford B D, Ward R C C and Wells M R 2001 *Appl. Phys. Lett.* **78** 964

Bentall M J, Cowley R A, Buyers W J L, Tun Z, Lohstroh W, Ward R C C and Wells M R 2003a *J. Phys.: Condens. Matter* **15** 4301–30

Bentall M J, Cowley R A, Ward R C C, Grier E J and Wells M R 2003b *J. Phys.: Condens. Matter* **15** 6493–512

Bowden G J, Beaujour J-M L, Goordeev S, de Groot P A J, Rainford B D and Sawicki M 2000 *J. Phys.: Condens. Matter* **12** 9335–46

Bowden G J, Beaujour J-M L, Zhukov A A, Rainford B D, de Groot P A J, Ward R C C and Wells M R 2003 *J. Appl. Phys.* **93** 6480

Bowden G J, Martin K N, Rainford B D and de Groot P A J 2008 *J. Phys.: Condens. Matter* **20** 015209

Brown W F 1963 *Micromagnetics* (New York: Interscience) p 143

Choi Y, Jiang J S, Pearson J E, Bader S D, Kavich J J and Freeland J W 2007 *Appl. Phys. Lett.* **91** 072509

Cullity B D 1972 *Introduction to Magnetic Materials* (Reading, MA: Addison-Wesley) See p 402 for a discussion of Brown's paradox

Dumesnil K, Dufour C, Mangin Ph, Fitzsimmons M R, Park S, Rhyne J J, Rogalev A and Borchers J A 2005a *J. Appl. Phys.* **97** 10K108-1

Dumesnil K, Dufour C, Mangin Ph, Rogalev A and Wilheim F 2005b *J. Phys.: Condens. Matter* **17** L215

Dumesnil K, Dutheil M, Dufour C and Mangin Ph 2000 *Phys. Rev.* B **62** 1136

Fitzsimmons M R, Park S, Dumesnil K, Dufour C, Pynn R, Borchers J A, Rhyne J J and Mangin Ph 2006 *Phys. Rev.* B **73** 134413

Jiang J S, Pearson J E, Liu Z Y, Kabius B, Trasobares S, Miller D J, Bader S D, Lee D R, Haskel D, Srajer G and Liu J P 2004 *Appl. Phys. Lett.* **85** 5293–95

Jiang J S, Pearson J E, Liu Z Y, Kabius B, Trasobares S, Miller D J, Bader S D, Lee D R, Haskel D, Srajer G and Liu J P 2005 *J. Appl. Phys.* **97** 10K311

Martin K N, de Groot P A J, Rainford B D, Wang K, Bowden G J, Zimmermann J P and Fangohr H 2006 *J. Appl. Phys* **101** 09K511

Sawicki M, Bowden G J, de Groot P A J, Rainford B R, Beaujour J-M L, Ward R C C and Wells M R 2000 *Phys. Rev.* B **62** 5817–20